

Tunneling through Either Intact, or Jointed, or Faulted Rock

N. R. Barton

NB&A, Oslo, Norway

ABSTRACT: Rock masses obviously represent the most variable of engineering materials, and the three categories listed in the title represent most of the range of rock quality. We need to include stress magnitudes, water pressure and permeability to be more complete, but will ignore swelling pressures. This keynote paper will address some new findings about tunneling through these three categories. For instance, the critical tangential stress experienced when fracturing of intact rock initiates in deep tunnels is caused by the ratio of tensile strength/Poisson's σ_t/ν . This explains the critical ratio $\sigma_\theta/\sigma_c \approx 0.4$. The extensional strain-induced fracturing will mostly propagate in shearing mode at higher stress levels, and this can be the source of rock bursts. The presence of jointing helps to dissipate the latter. Contrary to the experiences with drill-and-blast tunneling, TBM experience difficulties at both ends of the spectrum (intact, jointed, faulted). Partly for this reason, deceleration from day to week to month to one year is a common experience, also shown by the remarkable world records of TBM performance. A simple formula explains the delays of TBM tunnels in fault zones.

1 THE ROCK THAT BEARS THE LOAD

When we excavate a tunnel through intact, jointed or faulted rock masses, with Q-values potentially ranging from 1000 to 0.001, how important is the capacity of the support and reinforcement of the tunnel periphery, compared to the capacity of the surrounding 'cylinder' of rock mass to take load? The redistributed stresses, and the slightly deforming and adjusting rock blocks in the surrounding 'cylinder' (with dimensions which may be up to several tunnel diameters in thickness), account for a huge majority of the load-bearing abilities, except when very close to the surface.

The shotcrete, rock bolts, and occasional concrete of single-shell NMT (Q-system-based) tunnels, are selected merely to retain the load bearing abilities of the all-important surrounding rock mass. Naturally we can assist this process with sufficiently high-pressure pre-injection, if using stable (non-shrinking and non-bleeding) microcement suspensions. It is believed that most of the six Q-parameters are effectively improved by correctly carried-out high-pressure pre-injection. We know of velocity increases and permeability tensor rotations and magnitude reductions, even as a result of quite conservative grouting in dam abutments (Barton, 2012a). Hydraulic (e) and physical apertures (E) must be differentiated.

Even the thickest concrete lining can hardly compete with the hundreds or thousands of tons of load that are arched around each running meter of a tunnel. For instance, a 5MPa vertical stress at 200m depth, which may be concentrated to more than 10MPa in the tunnel walls, arch or invert (depending on the stress anisotropy) causes variation from 1,000 to 500 tons/m² in the nearest meter-thick-meter-wide, naturally load-bearing 'rock-mass-ribs' which surround the excavation. In the first 10m of the surrounding rock 'cylinder' an estimated load-in-the-arch of 5,000 to 10,000 tons per running meter of tunnel, obviously far exceeds the load-bearing abilities of shotcrete, rock bolts or concrete. At 1,000m depth the load-bearing capacity of the natural rock arch is even more essential.

The 'softest' support of all, the lattice girders used in NATM tunneling, have little to contribute in hard rock with marked over-break, because good contact with the tunnel perimeter is difficult. Why do we seldom see over-break and its volumetric (and stress-distribution) consequences in drawings and numerical models of concrete-lined NATM tunnels?

In both single-shell NMT and double-shell NATM philosophies, we are attempting to *help the rock to help itself*. Clearly there are potentially big cost differences depending on how we do this, but these will not be addressed

as some technical tunneling matters are of more immediate interest. Specifically, how do intact, jointed and faulted rock masses impact both drill-and-blast and TBM tunneling, when at shallow depth, and when at great depth?

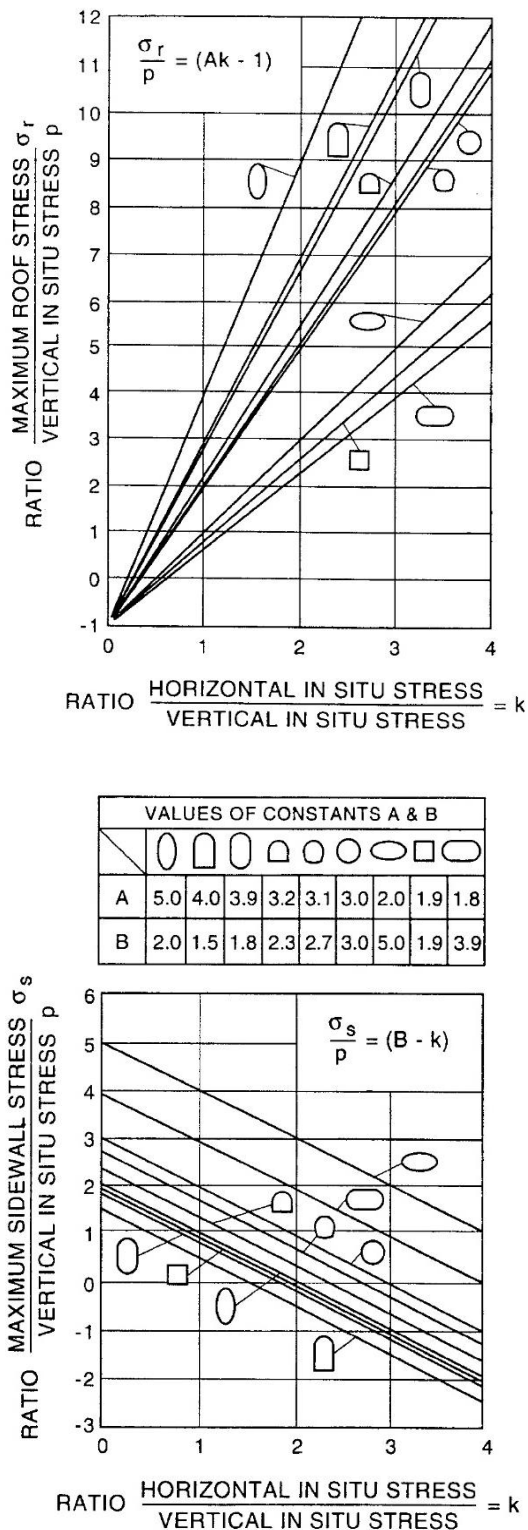


Figure 1. Theoretical (2D) stress concentration factors for tunnels and caverns of various shapes, excavated in unjointed isotropic elastic media. Hoek and Brown, 1980.

2 FRACTURING OF INTACT ROCK

For a circular tunnel driven in idealized intact, elastic, isotropic rock we can use the Kirsch assumption that $\sigma_{\theta \max} = 3\sigma_1 - \sigma_3$ and $\sigma_{\theta \min} = 3\sigma_3 - \sigma_1$. For more general excavation shapes, we can utilize the helpful diagrams of Hoek and Brown, 1980, which are reproduced in Figure 1. For a circular opening at 1,000m depth, with assumed σ_1 and σ_3 magnitudes of 30MPa and 15MPa, we would be looking at theoretical (intact, isotropic elastic medium) maximum and minimum tangential stresses of 75 MPa and 15 MPa.

It is helpful to view the details of stress concentration around circular openings using more realistic UDEC-BB models. Figures 2a and 2b illustrate two differently jointed models of a TBM access ramp for a previously planned UK ILW/LLW nuclear waste repository at Sellafield. (Barton, 2000). Note that despite the presence of some jointing there is a clear tendency for high tangential stresses to act around parts of the bolted, 8m span tunnels. However, the simulated jointing tends to dissipate the highest stress concentrations, and maxima of 56MPa and 30MPa are predicted in these two models, representing interbedded sandstones and siltstones at 300m depth, and welded tuff at 650m depth. The thickest sandstone bed is the cause of the high stress in the invert in Figure 2a. When comparing stress/strength in the traditional way, some ‘stress-induced’ fracturing might be predicted, though unlikely in the tuff.

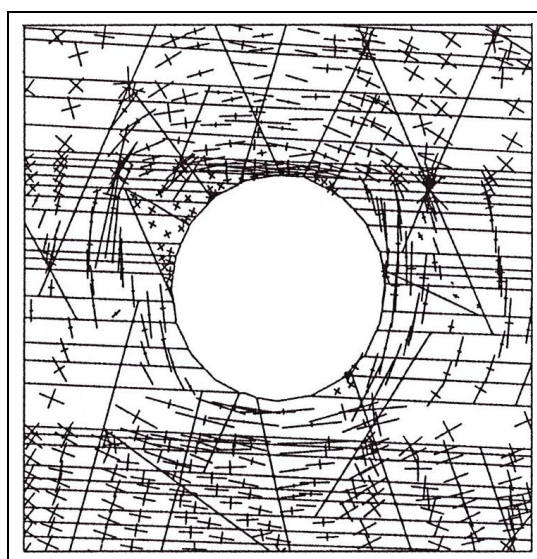


Figure 2a. UDEC-BB distinct element model of a TBM spiral access tunnel. Chryssanthakis, 1991. The maximum tangential stress reaches 56 MPa in the sandstone invert.

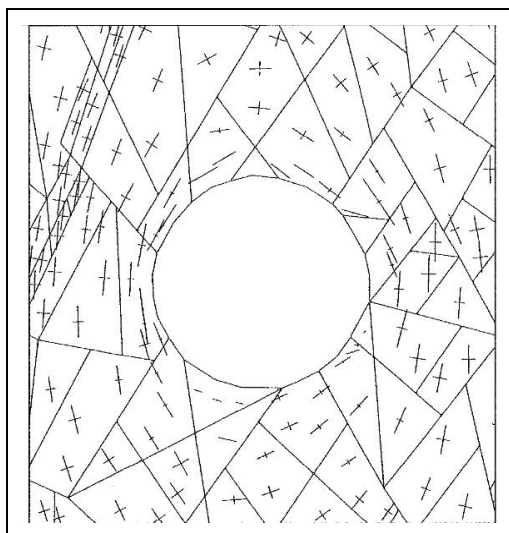


Figure 2b. UDEC-BB distinct element model of a TBM spiral access tunnel. Hansteen, 1991. The maximum tangential stress reaches 30MPa in the left wall. The jointing represents the welded tuff of the BVG ignimbrite.

In the three previous examples of maximum tangential stress: 75MPa: ideal unjointed, 56MPa: thick sandstone bed, and 30MPa in the left wall of the tunnel in welded tuff, a logical next design step would be to compare these values with a distribution of (or minimum) UCS value. This would be to check if the stress/strength ratio $\sigma_{\theta \max} / \sigma_c > 0.4$, signifying the possible onset of ‘stress-induced fracturing’. In the Q-system, for single-shell NMT tunnel support consisting of permanent B+S(fr) (Barton and Grimstad, 2014), this would mean selection of a higher SRF value, and a lower Q-value, therefore requiring heavier support.

When using the Q-system assessment of the SRF factor we would examine the following table, which was derived by Grimstad and Barton, 1993 and is based on Grimstad’s numerous observations in deep Norwegian road tunnels which exhibited ‘stress-induced’ fracturing, popping and bursting.

Table 1. SRF (stress reduction factor) in the Q-system rating tables (Table 6 of Grimstad and Barton, 1993). Note the strong acceleration of SRF when the stress/strength ratio $\sigma_{\theta \max} / \sigma_c$ exceeds 0.4 to 0.5.

| b) Competent rock, rock stress problems | σ_c / σ_1 | $\sigma_{\theta} / \sigma_c$ | SRF |
|---|-----------------------|------------------------------|---------|
| H Low stress, near surface, open joints. | > 200 | < 0.01 | 2.5 |
| J Medium stress, favourable stress condition. | 200-10 | 0.01-0.3 | 1 |
| K High stress, very tight structure. Usually favourable to stability, may be unfavourable for wall stability. | 10-5 | 0.3-0.4 | 0.5-2 |
| L Moderate slabbing after > 1 hour in massive rock. | 5-3 | 0.5-0.65 | 5-50 |
| M Slabbing and rock burst after a few minutes in massive rock. | 3-2 | 0.65-1 | 50-200 |
| N Heavy rock burst (strain-burst) and immediate dynamic deformations in massive rock. | < 2 | > 1 | 200-400 |

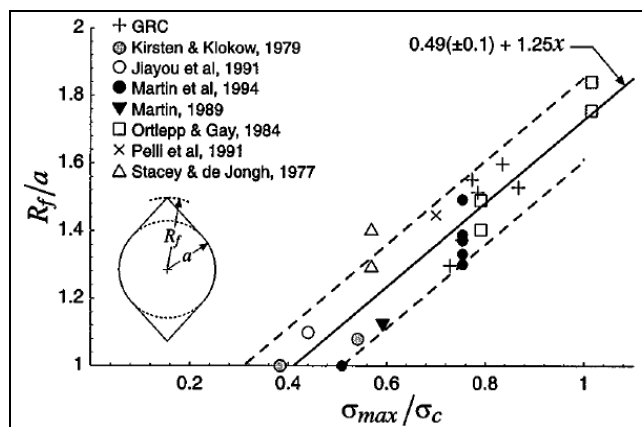


Figure 3. Observations of failure initiation and depth of ‘stress-induced’ over-break, after Martin et al. (1999).

The above is the traditional way to assess the likelihood of ‘stress-induced’ fracturing. It is supported (independently) by a later compilation of mining and nuclear waste URL research, published by Martin et al. (1999), reproduced in Figure 3. This also shows the associated approximate depth of ‘stress-induced’ ‘dog-earing’ or break-out, when the stress/strength ratio exceeds 0.4 (+/- 0.1).

We observe that the common ratios of stress/strength for spalling are in the range of 0.3 - 0.5, with a medium value of approximately 0.4. In reality, the critical ‘stress/strength’ ratio of 0.4 is related to *critical tensile strain*, and the typical ratios of σ_c / σ_t (about 10) and Poisson’s ratio (about 0.25). Barton and Shen, 2017, explain the new extension strain theory in more detail, and give FRACOD modelling examples.

Table 2. The extensional strain logic of Dr. Baotang Shen explains the critical ratio of stress/strength = 0.4 (+/- 0.1).

| | |
|---|---|
| $\epsilon_3 = [\sigma_3 - \nu (\sigma_1 + \sigma_2)] / E$ (3D stress/strain) | $\epsilon_3 = [\sigma_3 - \nu \cdot \sigma_1] / E$ (2D stress/strain) |
| When $\nu (\sigma_1 + \sigma_2) > \sigma_3$, negative extension strain $(-\epsilon_3)$ will occur. | When $\nu \cdot \sigma_1 > \sigma_3$, negative extensional strain $(-\epsilon_3)$ will occur. If $(-) \epsilon_3 > (-) \epsilon_c$ (critical) tensile failure occurs $-\epsilon_{crit} = \sigma_t / E$ |
| At the tunnel wall, $\sigma_3 = 0$, and $\sigma_1 = \sigma_{\max. \text{ tang. stress}}$ Therefore $(-) \sigma_t / E = \epsilon_c = (-) (\nu \cdot \sigma_{\text{tang. critical}}) / E$ (Next: eliminate common Young’s modulus E) | |
| $\sigma_{\text{crit. tang. stress}} = \sigma_t / \nu \approx$ | $\frac{UCS}{10\nu} = \frac{UCS}{10 \times 0.25} = 0.4 \times UCS$ |

Due to typical ratios of σ_c/σ_t (or UCS/σ_t) ≈ 10 , and typical values of Poisson's ratio ≈ 0.25 , the commonly occurring onset of extensional failure (and acoustic emission in a laboratory triaxial test) is when reaching an axial (i.e. 'tangential') stress $\approx 0.4 \times UCS$. Both in a triaxial test and around a circular tunnel, the initial extensional strain-induced tensile fracturing will tend to coalesce and propagate in *unstable shearing*. The FRACOD (fracture mechanics based Boundary Element) models which follow later, show initiation of fracturing by extensional strain mechanisms, followed by propagation by (unstable) Mode II shearing. It is the latter which may cause rock bursting.

3. REAL FRACTURING AND SOME MODELLING

One of the very earliest successful TBM tunneling projects is accorded to Beaumont. Thanks to a 'precedent conditions' legal case at the UK-France Channel Tunnel in the 1990's, the writer had the opportunity to inspect the 2.2m diameter 'pilot tunnel' together with Geo Engineering. This was driven in 1880 in the same chalk marl. A photograph of a 'stress-induced' (or perhaps extension-strain induced) failure is shown in Figure 4. The reason is two-fold. The chalk marl had a UCS in the range of only 4 to 9 MPa, and at this point passed beneath a 70m high chalk cliff on the south coast of England. Perhaps σ_1 was ≈ 1.5 MPa.

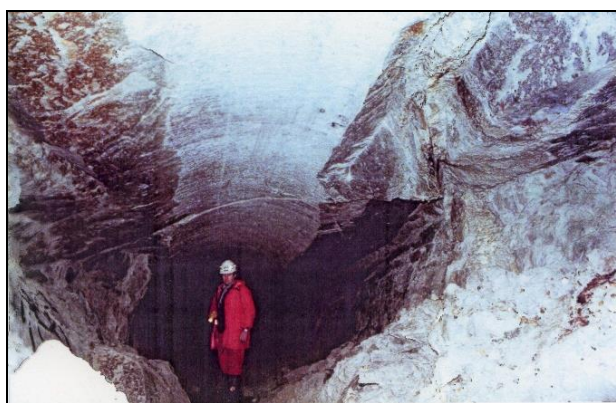


Figure 4. A stress (or strain) induced failure zone in the 1980 Beaumont Tunnel driven in massive chalk marl. At this location the tunnel curved beneath a 70m high chalk cliff. The 1.5 to 2MPa increment in the vertical stress, in the presence of a presumed low horizontal stress (assumed $k_0 \approx 0.33$) was sufficient to cause this fracturing. One bedding plane is visible in the arch, otherwise the chalk marl is quite massive in this location. A FRACOD model of the possible situation is shown in Figure 5.

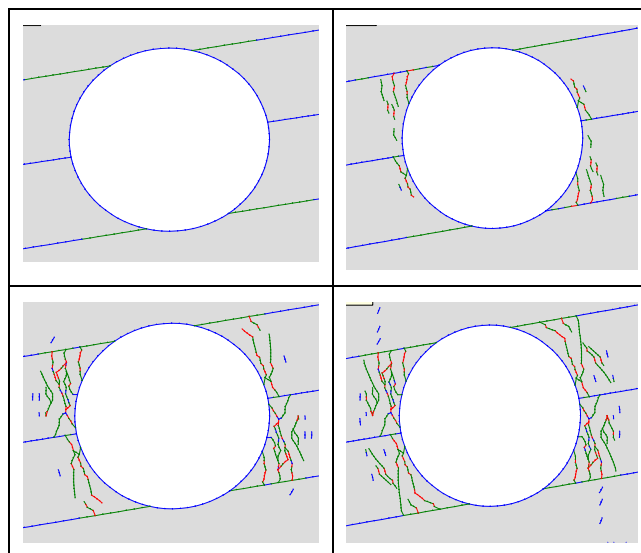


Figure 5. A FRACOD fracture-propagation model (Shen et al., 2014) of the Beaumont Tunnel cliff-loading situation with assumed $k_0 = 0.33$. Two other models performed by Dr. Shen with higher k_0 did not show such a good match with the failure. Barton, 2016.

In the late 1980's the writer was responsible for an NGI Joint Industry investigation of well-bore stability for various petroleum companies. Using 0.5x0.5x0.5m blocks of a model sandstone of $UCS = 0.5$ MPa, it was possible to drill in any direction in relation to a flat-jack-applied polyaxial stress. Due to the deliberately high loading, to simulate deep wells, the only mode-of-failure observed was the classic log-spiral of Bray (1971). Figure 6 shows examples.



Figure 6. Log-spiral fracture propagation in shear, which is unstable, and may be typical of the highest σ_{max}/σ_c data shown in Figure 3. See Addis et al. (1990) for details.

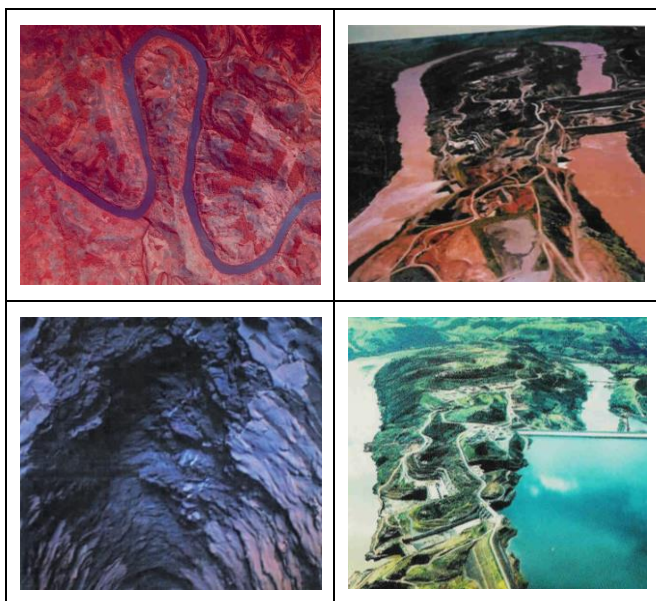


Figure 7. An 11 km loop in the Uruguay River in SE Brazil was the site of the 1,400 MW Ita HEP. Extremely high NNW-oriented horizontal stresses caused ‘stress-induced’ fracturing and tensile cracking in a total of nine tunnels crossing through the most massive ($Q>100$) basalt flows. Near-surface stresses also fractured the spillway.

The diversion tunnel (one of five) shown in Figure 7 measured 14 x 16 m, and the depth of break-out was 2 to 3m, even more in the invert. The ratio of $\sigma_{\theta \max} / \sigma_c$ was ≈ 0.65 according to depth of break-out, so the k_0 value may have been in the extreme range of 20 to 25, since UCS was ≈ 200 MPa, and the tunnels were shallow. Only where the five diversion tunnels and five pressure tunnels passed through the two *most massive* basalt flows was there fracturing or cracking. As we shall see in the FRACOD models that follow, jointing may have an important stress (and strain) dissipating role.



Figure 8. Stress (or strain) induced fracturing in massive marble at the Jinping II HEP project in China. Three TBM tunnels were later affected by serious rock-bursting, and drill-and-blast was the final solution for completing the project, due to several kilometers at 2.5km depth.



Figure 9. Stress (or strain) induced fracturing in massive marble at the Jinping II HEP project in China, where two of the four headrace tunnels were drill-and-blasted, but all tunnels had eventually to be completed by drill-and-blast due to the extreme depth along several kilometers of the 16.7km long tunnels. Sadly there were many fatalities.

Basically there was insufficient rock strength (UCS ≈ 60 -90 MPa) to avoid bursting at the Jinping II project, and regrettably the relative minimizing of an EDZ with TBM tunnelling puts the highest tangential stresses (too) close to the perimeter of such smooth-walled tunnels. Even the ratio of σ_1 / σ_c was as high as 1.0, so $\sigma_{\theta \max} / \sigma_c$ would be close to the top of Figure 3 data, i.e. in unstable shear propagation and therefore rock-burst territory.

4 DISSIPATING EFFECT OF JOINTING

The writer was involved as a consultant at the deep Olmos Tunnel planned to penetrate the Andes, back in 2004 and 2005. The new project to complete the Olmos Tunnel by TBM had not started. Stress levels at 1km and 2km depth in the Andes were not known, nor was there reliable observations of jointing, from a much earlier Russian drill-and-blast project. Figure 10

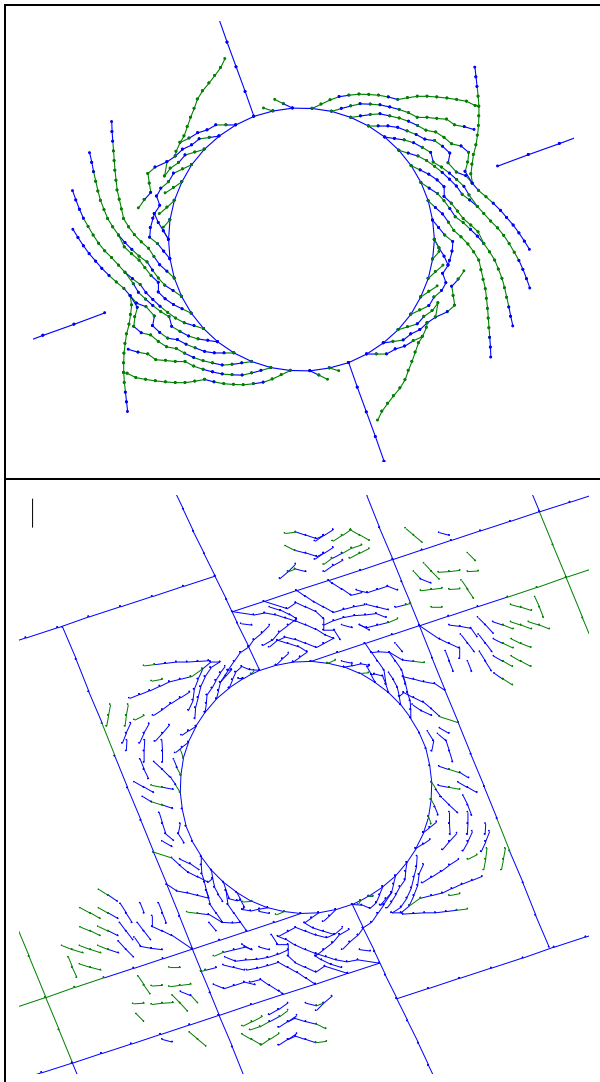


Figure 10. FRACOD modelling performed by Shen, 2005. The two cases shown demonstrate two different aspects. Firstly there is likely to be relatively undisturbed log-spiral shearing when the rock mass is massive with negligible jointing, if stress levels are sufficiently high. This is unstable and rock-burst producing when in hard brittle rock. Secondly the presence of even moderate jointing ‘disturbs’ the propagation in shear. Nevertheless there were eventually many rock burst experiences with 1 to 3m of ejected material above and in front of the Olmos TBM. The above exploratory models had: Top: $\sigma_v = 55\text{MPa}$, $\sigma_h = 40\text{MPa}$. Bottom: $\sigma_v = 30\text{MPa}$, $\sigma_h = 60\text{MPa}$.

shows some of the exploratory modelling performed at that time. More distinctly jointed models using UDEC were also performed to explore further behavioural possibilities. In fact such deep TBM tunneling was not advised, but the advice came contractually too late. In a subsequent keynote lecture, which had the benefit of further FRACOD modelling by Shen, Barton and Shen (2016) showed specific examples of the ‘positive effect’ of jointing in

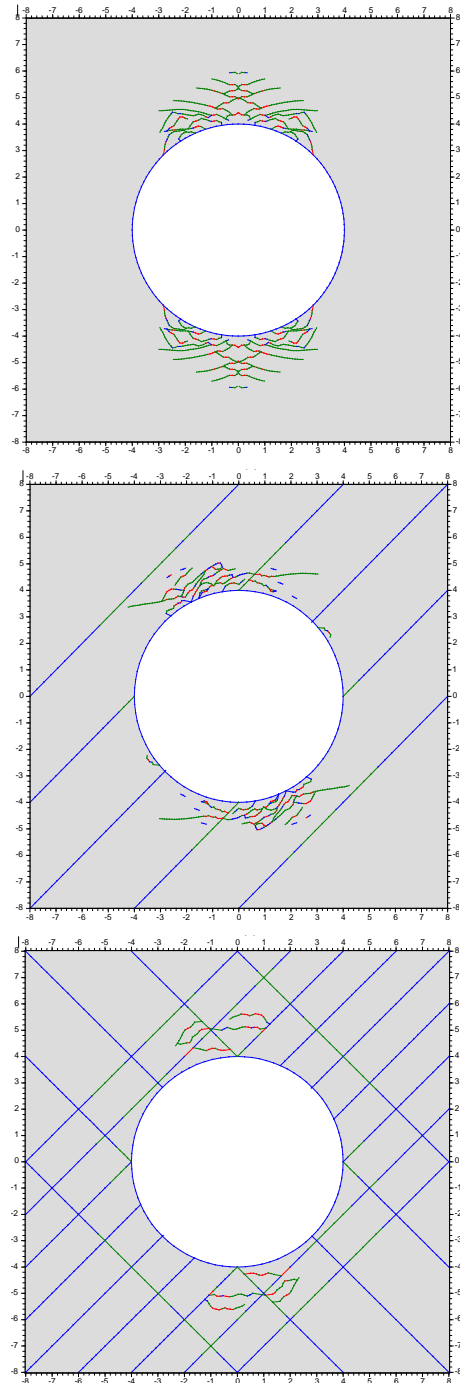


Figure 11. FRACOD modelling of the energy dissipating effect of one and two joint sets, when 1,000m deep TBM tunneling was simulated. Barton and Shen (2016).

simulated TBM tunnels at 1km and 2km depth. Some results of 1km deep simulations are shown in Figure 11. Boundary stresses assumed: $\sigma_{Hmax} = 50\text{MPa}$; $\sigma_v = 25\text{MPa}$. The rock properties assumed for several such models were the same as for the well-researched Äspö diorite, as listed with Finnish data in Siren (2012). For the base case, the strength and fracture toughness of the rock were: UCS = 165MPa; cohesion $c = 31\text{MPa}$; internal friction

angle $\phi = 49^\circ$; tensile strength $\sigma_t = 14.8\text{MPa}$; mode I fracture toughness $K_{IC} = 3.8 \text{ MPa m}^{1/2}$ and mode II fracture toughness $K_{IIC} = 4.7 \text{ MPa m}^{1/2}$ (Siren, 2012). The maximum tangential stress at the tunnel was calculated to be $\sigma_{\max} = 150\text{MPa}$, and the ratio of $\sigma_{\max}/\sigma_c = 0.75$. Based on Martin, Kaiser and McCreath (1999), the depth of tunnel failure (from Figure 3) is $R_f/a = 1.3-1.5$.

5 JOINTING, SHEARING, OVER-BREAK

As we move from tunneling in mostly intact rock, to tunneling in jointed rock, there are of course new issues to address. The properties of the jointing, and their reaction to the shear stresses caused by excavation become important. We can start by thinking through the effect of the number of joint sets on the drilling-and-blasting process: how much over-break may occur beyond the planned cross-section?

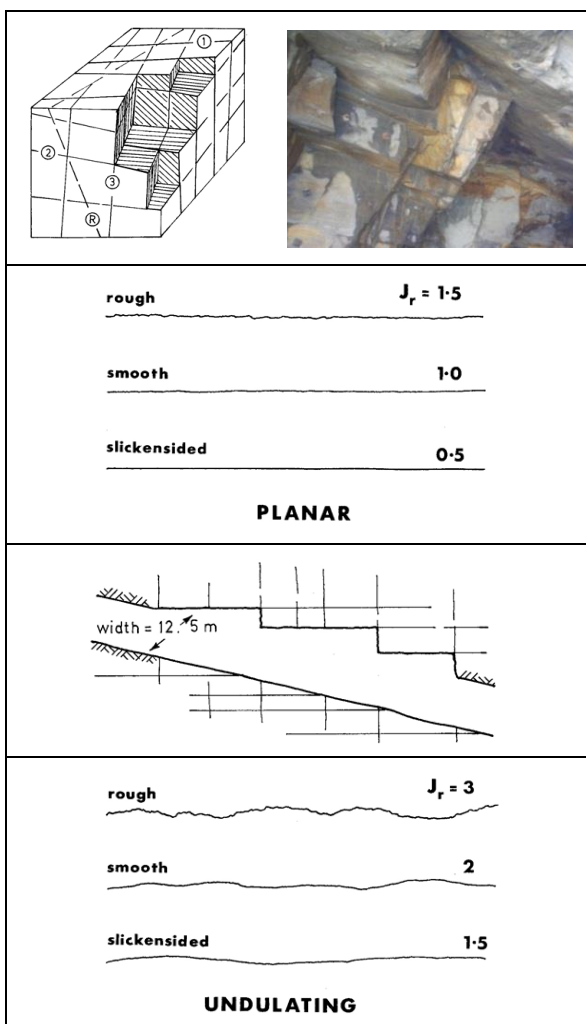


Figure 12. Over-break criterion using an unconventional Q-system based ratio $J_n/J_r \geq 6$ (Barton, 2007).



Figure 13. Major break-out and wedge collapses caused by structural geologic details including major discontinuities with adverse shear strength, including slickensided surfaces, e.g. low ratios of J_r/J_a .

The ratio J_n/J_r suggested by Barton (2007) has recently been used by some contractors in tunnel claims. For instance: 6/0.5, 9/1, 9/1.5, 12/2, 12/1.5 cause over-break due to insufficient joint roughness. However, if roughness is sufficient even three sets plus random, or even four sets may not allow over-break, as $15/3 < 6$.

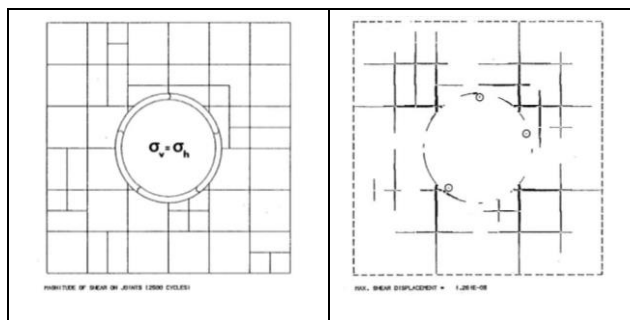


Figure 14. A UDEC-BB simulation of a circular (TBM) tunnel with equal boundary stresses ($k_0 = 1.0$). Joint shearing in '45° sectors' is nevertheless experienced despite the stress isotropy. Christianson (1985).

The above UDEC-BB modelling (Figure 14), was performed by Christianson, of Itasca just after installing the BB joint behaviour subroutine in UDEC while at NGI in 1985. It is perhaps a surprise to see joint shearing, even when isotropic stress is applied. Shen and Barton (1997) showed that this is an important part of the inevitable EDZ. The Mohr-Coulomb based analyses shown in Figure 15 again reinforce the philosophy (and reality) presented in the introduction, that tunnelling causes effects in the rock mass that are not controlled by, and do not need to be controlled by, the support and reinforcement, whether economic single-shell NMT (B+Sfr, maybe + RRS) or more expensive double-shell NATM (B+Smr+LG+CCA).

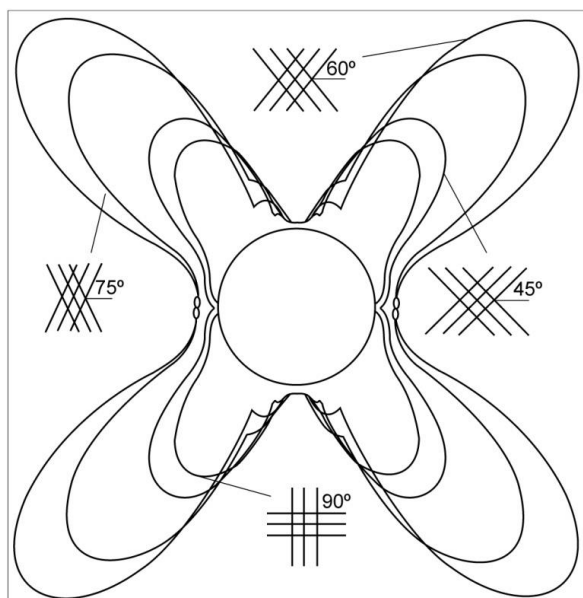


Figure 15. The theoretical zones of joint shearing when four different intersecting joint patterns are modelled by Mohr-Coulomb analysis. Applied stress is strongly anisotropic, $K_0 = 1/4$, but $\phi = 40^\circ$ (Shen and Barton, 1997). Note kink-bands when blocks are small: Figure 17.

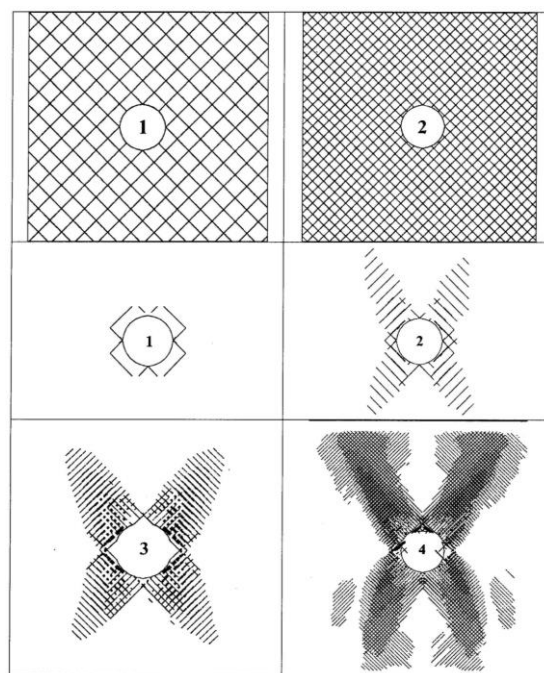


Figure 16. In these UDEC-MC models the block size has been successively halved. The 4th model has 10,000 blocks. Only joint shearing in excess of 3mm is shown. Shen and Barton (1997). The trauma caused by fault zones, where block size is usually much reduced, is easy to understand, especially when also clay and water pressure can cause the erosion of blocks (and therefore the trapping of TBM on occasion).

Concerning the need for tunnel support and reinforcement, the most important thing is that the perimeter of the tunnel is 'kept intact' either before over-break occurs (if using spiling or pipe-roof) or after 'geologic over-break has already occurred as in Figure 12. The economic strength of NMT is that the three examples of over-break illustrated in Figure 12, and each of the examples in Figure 13, do not need to be filled with concrete (or excessive shotcrete).

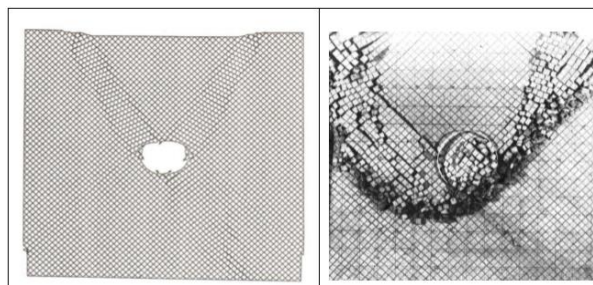


Figure 17. When block size is reduced, both in numerical and physical models, there is a strong likelihood of kink-band formation. This occurs more frequently with non-linear Barton-Bandis than with linear Mohr-Coulomb joint behavior. (Shen and Barton, 1997 and Barton and Hansteen, 1979).

6 SINGLE-SHELL NMT IN JOINTED ROCK

The Q-system was developed mainly from single-shell B+S and B+S(mr) case records in 1973, and since about 1986, also B+S(fr). (Grimstad and Barton, 1993). Cases now number in the thousands. Over the years the Q-system has developed its own essential place within the wider practices of NMT – the Norwegian Method of Tunnelling. The term was first coined in a multi-author, multi-company publication in 1992, as a deliberate differentiation of what 'NMT does' compared to NATM. (Barton et al. 1992). Huge numbers of tunnels, caverns and mines around the world utilize one or the other method, in one form or another, sometimes using RMR and Q.

| | |
|-----------------|---|
| Design | Preliminary design is based on field mapping, drill core logging and seismic interpretation. Final support is selected during tunnel construction based on tunnel logging and use of the Q-system support recommendations. |
| Support | The permanent support usually consists of high quality wet process, fibre reinforced shotcrete and fully grouted, corrosion protected rock bolts. |
| Contract | The owner pays for technically correct support. Needed support is based on the agreed Q-value, and may vary frequently. |









Figure 18. Some details concerning NMT. Tunnels are dry, drained, and PC-element cladded (a free-standing 'drip-shield' with outer membrane) if required for road or rail tunnel use. ('Pigging' = scaling).

The details described in Figure 18 date from an early 1990's Norwegian contractor brochure, and have remained basically unchanged, as the resulting tunnels, even with the optional free-standing cladding-and-membrane, are actually approximately ¼ of the price of a conventional double-shell NATM transport tunnel, if applied where there are high labour costs. Further differences between NMT and NATM are illustrated in Barton, 2017. A specific difference is that S(fr) was used in hydropower and road tunnels in Norway since 1979/1981. Figure 19 illustrates why, in NMT, it is preferred to S(mr).

In the last 20 years there is also more frequent use of high-pressure pre-injection in NMT transport tunnels, using stable, non-shrinking micro-cement and micro-silica to prevent environmental impact. This has been

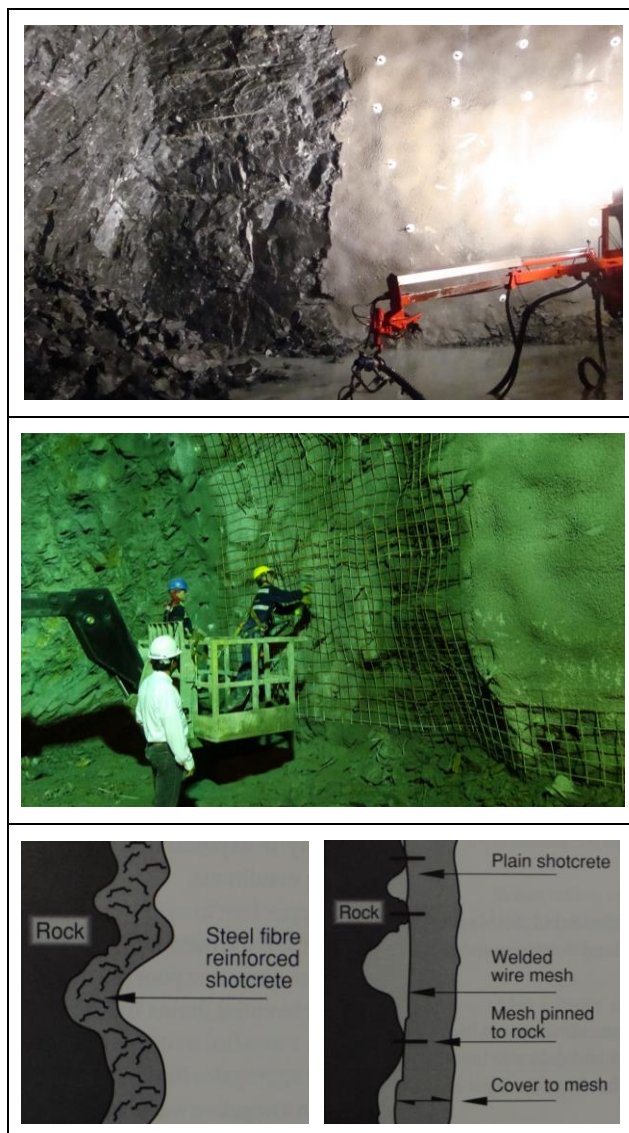


Figure 19. In single-shell NMT, where systematic bolting and fiber-reinforced shotcrete B+S(fr) are the norm, we gave up the use of S(mr) in the beginning of the 1980's. The reasons are clearly illustrated here, also with the help of the non-exaggerated sketches from Vandevall, 1996.

very successful, reducing inflow into the 'dry almost everywhere' 1 to 4 litres/ min/ 100m category. Occasional (< 0.001% ?) damp patches only. Examples are seen in Figure 20.

In Norwegian practice from the last 20 years there are good experiences using high pressure (5 to 10MPa) pre-injection. It should be noted that in Norway, we do not disqualify stable, non-bleeding micro-cements and micro-silica, by testing them with the filter pump, which demands artificial 'flow separation'. (Pers. comm. Dr. Steinar Roald). Also, based on careful experiments, the rule-of-thumb that $4x d_{95}$ is the minimum physical aperture in relation to (almost) maximum particle size is

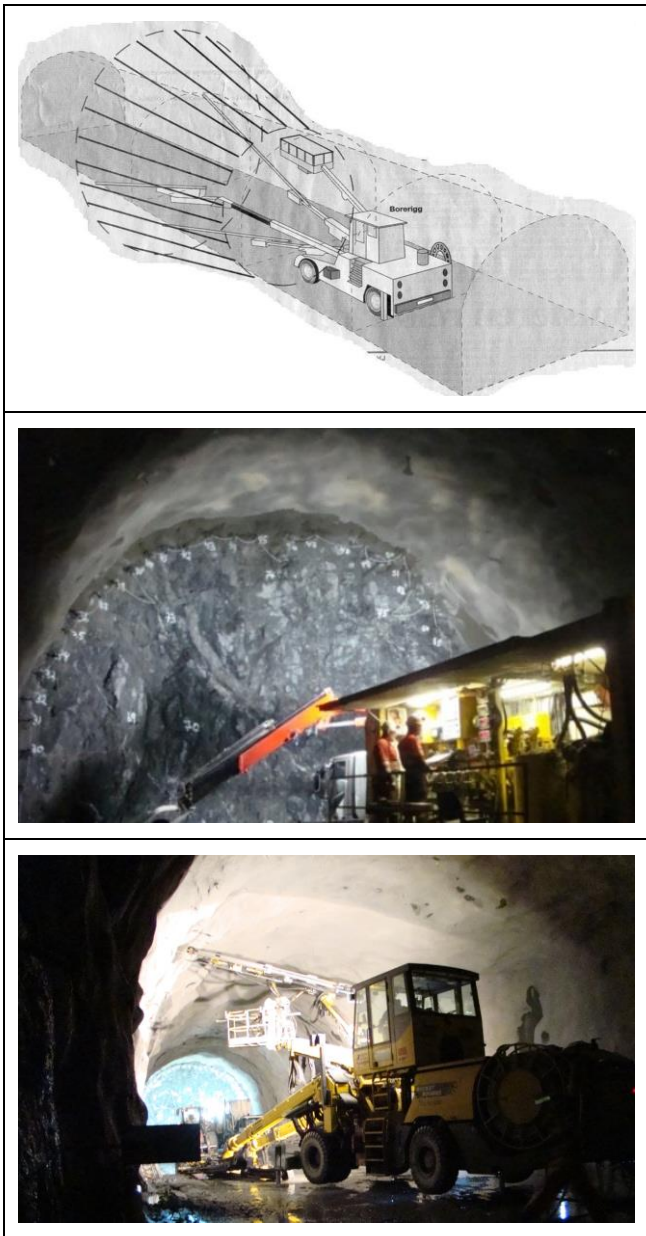


Figure 20. Pre-injection in the Bærum Tunnel of 5km length. Bottom: A single-point post injection is being carried out in an essentially dry 80m length of tunnel.

followed, compared to the strange opinion of the need for 10 to 12 x d_{95} seen elsewhere, as a presumed result of the erroneous filter pump test method.

7 OVER-BREAK NORMALLY NOT FILLED

An obvious point which needs emphasis for those not familiar with NMT is that whatever over-break occurs, due to structural geological reasons (the $J_n/J_r \geq 6$ criterion, Figure 12), or due to over-enthusiastic blasting, we do not fill the over-break (with concrete). Nevertheless the volume of S(fr) may be considerably increased.



Figure 21. Two extreme cases of over-break, seen in South America. Top: The top-heading of an adversely oriented cavern. Bottom: A too-shallow metro station. These strange cases are used here to emphasise that in NMT practice, if these were permanent excavations, there would be no attempt or need to fill the over-break with concrete. Q-system based B+S(fr) would be selected to ensure permanently stable excavations. A free-standing PC-element liner, bolted to the periphery, with external membrane could be used for the case of the station.

Figure 21 illustrates two extreme cases of over-break in order to emphasise the point that unintended over-excavation is not filled, nor needs to be filled with concrete (or more expensive shotcrete) when using NMT principles. The real road and rail tunnel over-break seen in poor-quality stretches of these tunnels in Figure 22 may have 8 to 10cm of S(fr) and (already covered) systematic bolting. In the case of the two-lane motorway tunnel, a free-standing liner and outer membrane ensure dry-but-drained conditions. Of course for the permanent support to be specified using the Q-system, as was the case in both tunnels, the engineering geologists from the owner and contractor have to be satisfied with the quality of the work. This includes high-pressure air-



Figure 22. Poor-quality (low-Q) sections of a road and rail tunnel, with resulting over-break and a very rough ‘finished’ appearance, following a probable 8 to 10cm of S(fr) and bolting. A free-standing liner, bolted to the rock, but with outer membrane, ensures a dry-but-drained road tunnel. The rail tunnel does not need this. It is also stable.

and-water washing of the tunnel arch and walls immediately prior to the planned shotcreting.

On the subject of differences between NMT single-shell and NATM double-shell tunnelling, (which Austrians are of the opinion is the norm), we may consider the challenges of supporting and reinforcing the 60m span arch of the Gjøvik cavern in the early 1990’s. Figure 23a illustrates the big arch (too large to see in its entirety from any one point). In Figure 23b, a section of the roof arch is seen, photographed from a distance of 20 to 40m. Note the 1m (approx.) over-break where there were probably local ratios of J_n/J_r of about 12/2 (three joint sets plus random and smooth but undulating $J_r = 2$ joints). There could have been 15/2 in places.

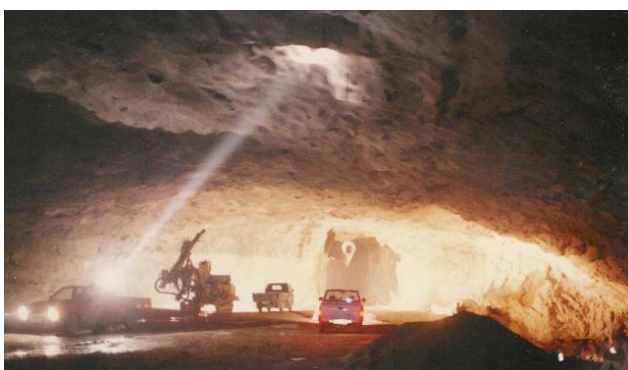


Figure 23a. The fully exposed 60m span arch of the Gjøvik cavern. This was a drained-but-dry single-shell construction, with permanent B + S(fr) consisting of 6m long bolts at 2.5m c/c and 10cm of S(fr). For security reasons twin-strand cables of 12m length and 5m c/c were also installed. Note the location of the cavern on the 1993 update of the Grimstad and Barton (1993) support chart.



Figure 23b. The jointed nature of the gneiss, seen during construction, with RQD = 60-90%, UCS = 90 MPa and $Q = 2$ to 30. A mean Q of 10 to 12 was obtained from logging of core from four boreholes and from systematic logging in the Gjøvik arch. Note the deep over-break beneath 10cm of S(fr) seen from a distance of about 25m.

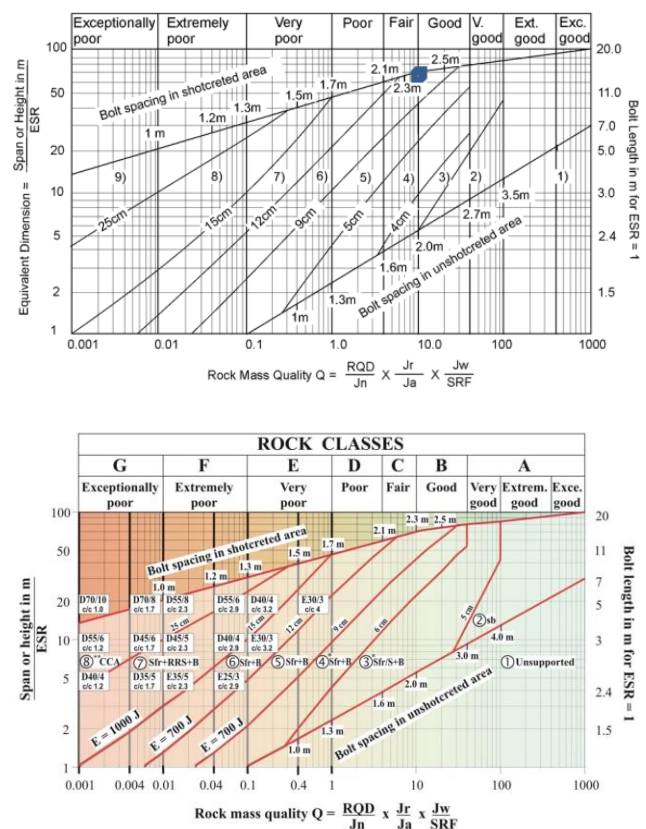


Figure 24. The Q-system tunnel-support-and-reinforcement charts from Grimstad and Barton (1993) and from Barton and Grimstad (2014). By far the dominant work in developing these charts and collecting case records was performed by co-author Grimstad. Note the dimensioning of rib-reinforced shotcrete arches, (RRS) for stabilizing extremely poor conditions. The boxes, with details such as [D45/6, c/c 1.7]: double layer of bars, 45cm total thickness, 6 bars, 1.7m c/c, are ‘located’ with their left sides along relevant Q-values, in this case an exceptionally poor $Q = 0.004$ and span ≈ 10 m. The construction of RRS is illustrated in Figure 25.

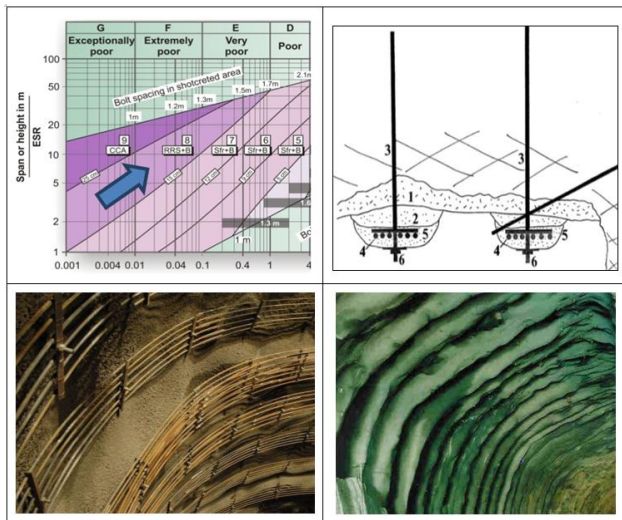


Figure 25. Some details of RRS features, which are far superior to lattice-girders (LG) due to the absence of (deformable) footings and the stabilizing presence of all-round bolting. The local filling of over-break with accelerated S(fr) prior to fixing the 16mm bars and bolting them to the shotcrete arch is an essential part of RRS.

Table 3. In summary, NMT is single-shell tunneling, with much reduced use of concrete since a sprayed shotcrete lining is normally used. Besides various important contractual elements (see multi-author descriptions in Barton et al., 1992) it consists of the following basic elements:

| |
|---|
| <i>Q-system logging for selecting close-to-the-face permanent support and reinforcement.</i> |
| <i>S(fr) steel or polypropylene fibre reinforced shotcrete. Typically 5 to 20 cm range of thickness.</i> |
| <i>B (utg) - CT-type with multiple corrosion protection. Typically 1.0 to 2.5 m c/c.</i> |
| <i>RRS (bolted and rib-reinforced shotcrete arches) when needed in rock masses with Q-values below 0.1.</i> |
| <i>Pre-grouting for dry tunnel, displacing water. Protects environment, prevents differential settlement damage to buildings founded on over-lying clays.</i> |
| <i>Free-standing, bolted PC-elements with outer membrane for dry tunnel, but allowing drainage. Gives improved 'finish' and lighting for main road tunnels.</i> |

It should be noted that lattice-girders (LG) should never be a part of Q-system designed NMT support, as they are considered the most deformable element of (NATM) tunnel support, and have demonstrated weakness when subjected to non-uniform loads, in other words when loaded by *unstable rock masses*, as opposed to unstable soils. The latter are likely

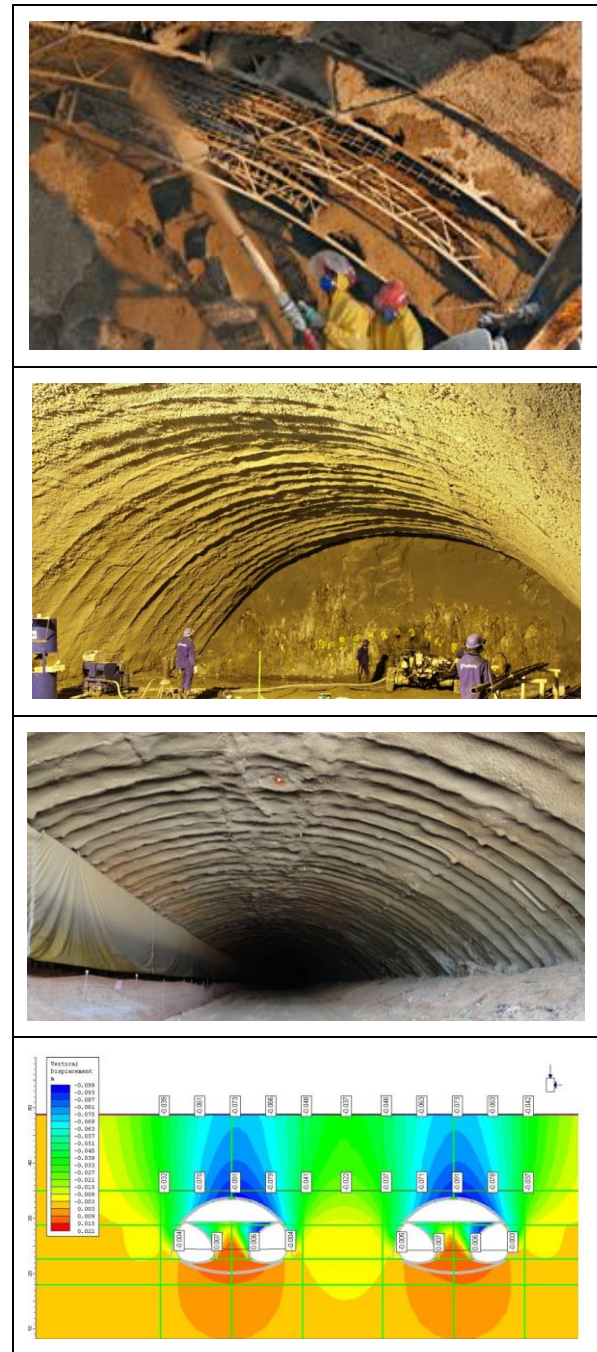


Figure 26 In each case illustrated, the LG failed due to unexpected non-uniform loading in jointed rock. Recently 2 x 140m of LG-supported NATM tunnel collapsed: first in the right-hand tube, then the adjacent left-hand tube.

to be more uniform in nature, helping the LG to perform as intended. Case records involving LG have never been part of the Q-system data base. Quite simply, LG are too deformable, and too susceptible to non-uniform loading in jointed rock. In soil and saprolite they may of course be, together with pipe-roof, the only solution, but loading may tend to be more uniformly distributed. Footings remain weak however.

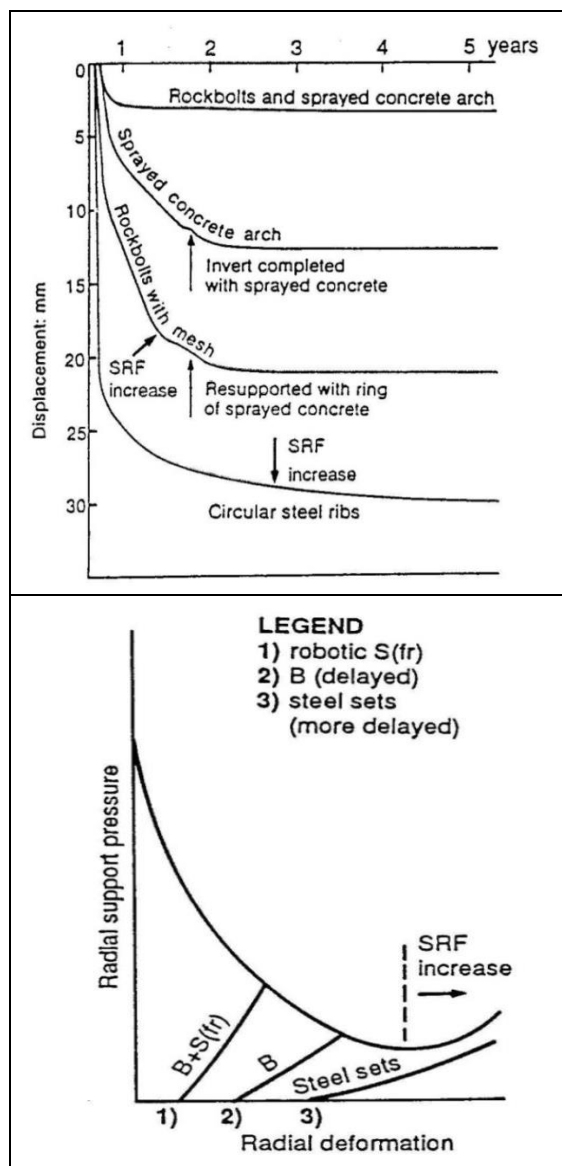


Figure 27 a and b. Figure 27a shows the four measured results of monitoring deformation behaviour for a period of five years in an experimental tunnel in mudstones, as reported by Ward et al., (1983). The circular steel ribs, similar in principle to lattice-girders, perform the worst, while even plain shotcrete and rock bolts perform admirably. The bottom diagram is from Barton and Grimstad, 1994, suggesting loosening and SRF increase.

Avoidance of steel sets (or lattice girders) remains an important advisory for NMT Q-system users. (See why in Figure 27). This advisory has not always been followed, even in Norway, and one may wonder at the confidence of those using unbolted free-standing structures. There have been some dramatic failures when unexpected loads have resulted from unstable rock masses, and the *isotropic loading assumptions*, as might be reasonable for soils, fail completely due to anisotropy and non-

uniformity in the case of jointed rock (with clay). The reasons for excluding LG for (temporary) support of tunnels in jointed rock are multiple:

1. It is difficult to make good contact between the tunnel (or cavern) perimeter and the lattice-girder, especially if there is deep over-break.
2. Rock mass deformation is needed to make 'solid' but only local contact with the steel. Rock mass strength may be reduced in the wrong places as a result.
3. When load starts to be applied by less stable parts of the excavation perimeter, the footings of the lattice girder will inevitably deform by a finite amount.
4. Strain and resulting stress must build up in the steel bars of the lattice girder for it to finally apply resistance to further deformation. Meanwhile the rock loosens.

In a large tunnel, one could roughly estimate that 25 to 50 mm of deformation might occur in this collective straining of the rock-lattice-girder combination, which as mentioned, also involves the (elephant) footing, with enlarged area for spreading load when in a temporary soft invert.

8 FAULT-ZONES THAT DELAY TBM

Tradition suggests that fault zones that delay drill-and-blast tunneling, such as that shown in Figure 28, are less well documented than the effects of fault zones that delay some TBM.

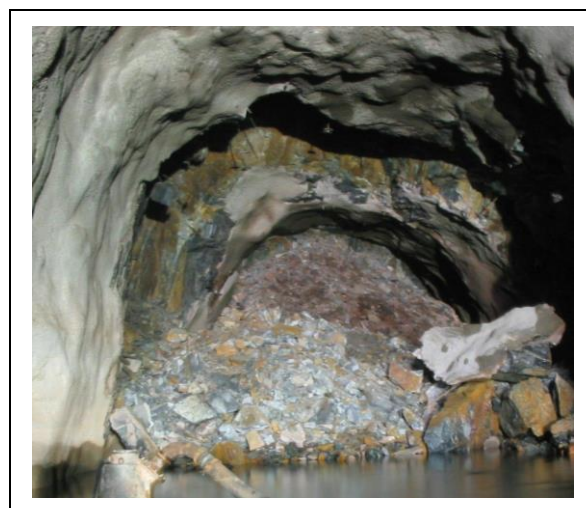


Figure 28. A fault zone delaying completion of an HEP tailrace tunnel in Brazil, one of five such features.

Fault zone delays in TBM tunneling can be deduced from performance data, because when fault-related delays occur there is often a very strong impact on the overall, and generally very fast performance. As shown in Figure 29 the so-called ‘unexpected events’, which are often experienced when no probe drilling is being performed, have a dramatic effect on the advance rate. They are often fault-related.

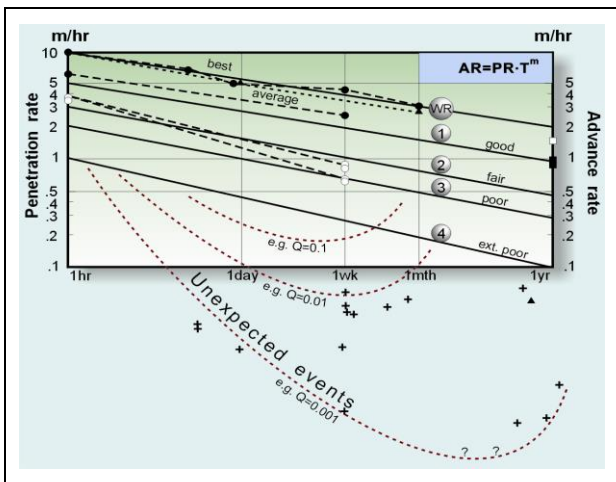


Figure 29. A synthesis of 1,000 km of mostly open-gripper TBM cases reported in Barton (2000). PR (m/hr) applies down the left axis. The remainder of the diagram shows log T versus log AR. WR shows world records.

The raw data from 145 TBM tunnels showed no horizontal performance lines. In other words the usual equation for TBM: $AR = PR \times U$ must have the relevant time-period defined. Does the quoted U apply to weekly or monthly performance? The sloping lines of performance represent *deceleration with time* (gradient -m). The remarkable set of TBM world records assembled by Robbins Company and synthesised by tunnel diameter in Figure 30 also show deceleration with time. (Barton, 2013).

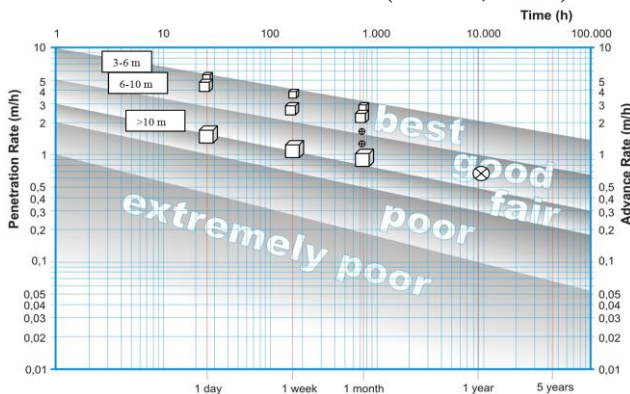


Figure 30. TBM world records plotted as log T – log AR. Note: world record D&B (O and X) LNS: 5.8km, 54 wks.

It appears that the TBM industry and designers of long (TBM) tunnels have not yet taken these trends seriously, and partly for this reason we see a fair number of TBM tunnels which are completed by drill-and-blast. A hybrid solution from the start may make much more sense, and can result in overall faster and cheaper long-distance tunneling. (Barton, 2012b, 2013).

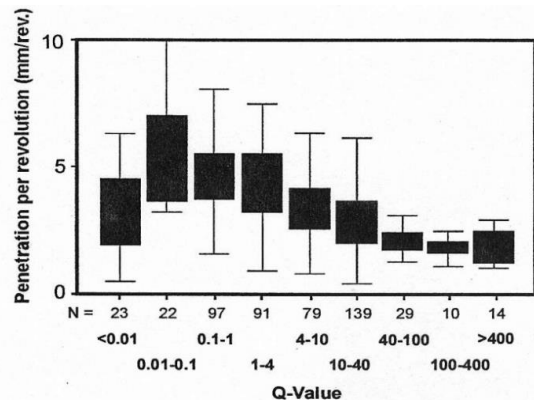


Figure 31. Recorded PR machine data (mm/rev) and Q-values logged behind the TBM, assembled ‘blind’ from 2.8km of a tunnel in granites in Malaysia. (Sundaram and Rafek, 1998). This PR-related data is of course somewhat different from the actual advance rate AR due to delays for support when the Q-value is very low. See Figure 32.

Figure 31 shows the Q-value based trends of penetration rate, expressed as mm/revolution. The relation between PR and Q, and between AR and Q are indicated in approximate terms in Figure 32. It is unfortunately true that TBM perform poorly at both ends of the Q-value spectrum. Note that the standard Q-system adjectives shown near the top of Figure 32 need to be modified for TBM. The more relevant TBM-related adjectives are shown in Figure 33.

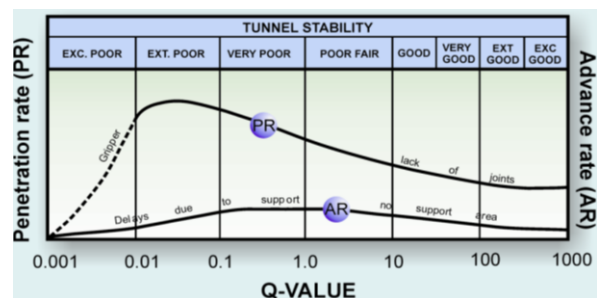


Figure 32. When TBM performance trends are set up in relation to Q-values, with machine-rock interaction parameters like cutter force and rock mass strength so far ignored, the PR and AP trends are roughly as shown.

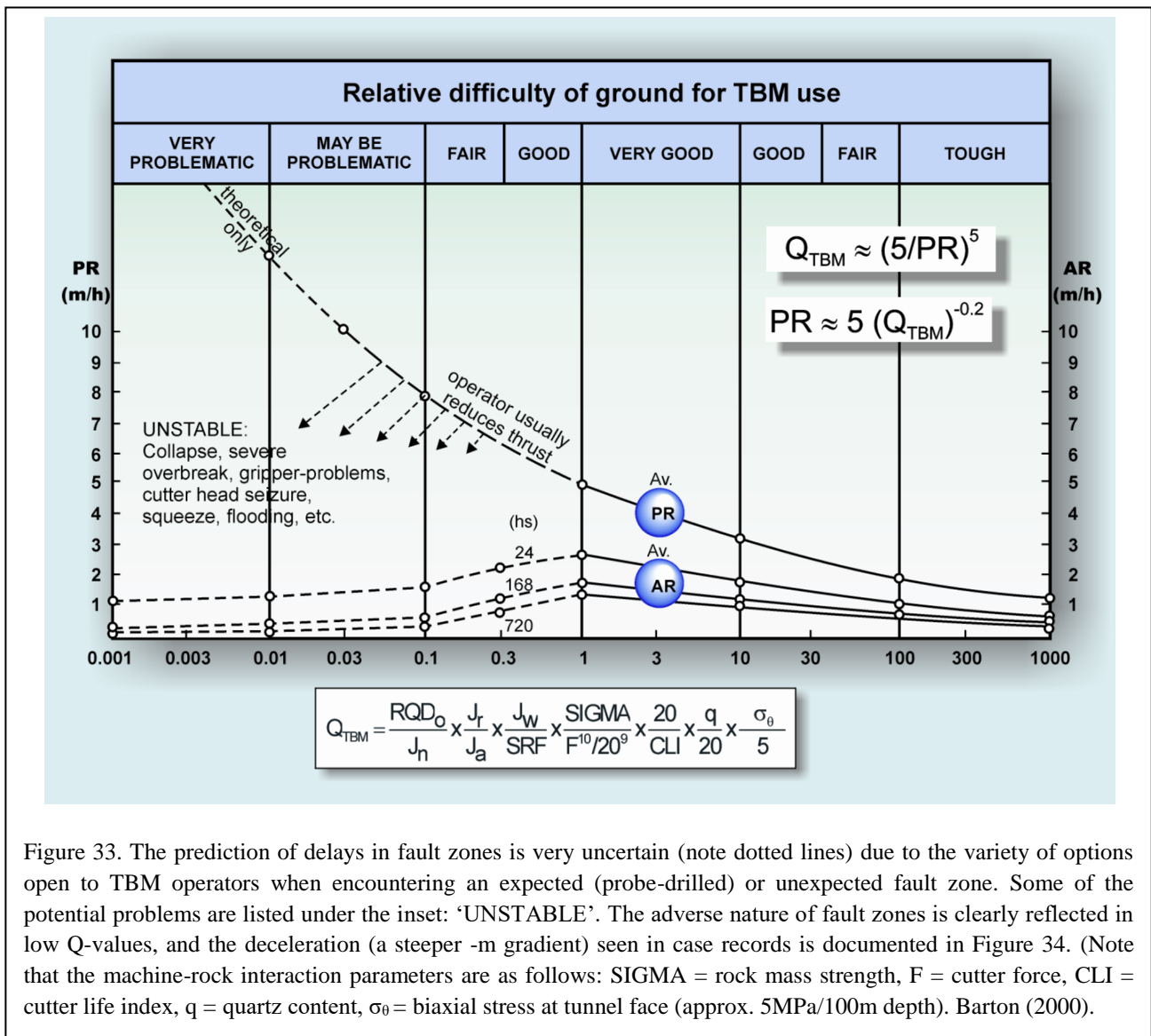


Figure 33. The prediction of delays in fault zones is very uncertain (note dotted lines) due to the variety of options open to TBM operators when encountering an expected (probe-drilled) or unexpected fault zone. Some of the potential problems are listed under the inset: ‘UNSTABLE’. The adverse nature of fault zones is clearly reflected in low Q-values, and the deceleration (a steeper -m gradient) seen in case records is documented in Figure 34. (Note that the machine-rock interaction parameters are as follows: SIGMA = rock mass strength, F = cutter force, CLI = cutter life index, q = quartz content, σ_{θ} = biaxial stress at tunnel face (approx. 5MPa/100m depth). Barton (2000).

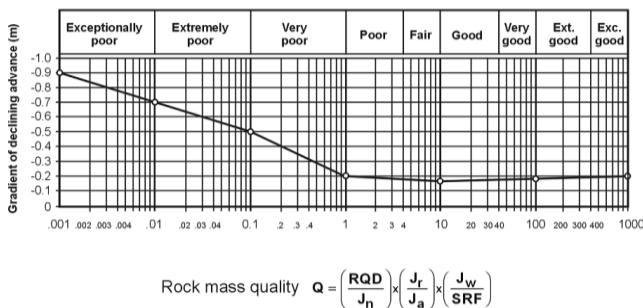


Figure 34. The regular Q-value, as opposed to the Q_{TBM} value shown in Figure 33, is seen to have a dramatic effect on the deceleration gradient (-m) of TBM, when low values of Q (e.g. < 0.1) are registered. It is assumed that new generations of TBM like cross-overs and ACT can help to ‘push the hill’ to the left, but they will not eliminate the adverse nature of serious faults unless pre-injection and drainage are successfully carried out. In all cases there will be delays, but possibly reduced delays.

The decelerations seen in all the TBM performance curves in Figures 29 and 30, a feature apparently almost universally ignored in TBM prognoses, happens to be the source of estimation of TBM delays in fault zones. It can be noted that the (-m) gradients of deceleration are strongly tied to low Q-values in Figure 34. This is empirical i.e. demonstrated by actual performance of TBM. Why fault zones delay TBM can be quantified as follows:

8.1 Fault-zone delays explained

We need three basic equations to understand potential delays in fault zones. (The following nomenclature will be used as before: AR= advance rate, PR= penetration rate, U= utilization, expressed as a fraction, for any chosen total time period T in hours). Firstly:

$$AR = PR \times U \tag{1}$$

(All TBM must follow this first equation).

$$U = T^m \tag{2}$$

(Due to the reducing utilization with time, the advance rate decelerates, so time T must be quoted. See Figures 29, 30 and 33).

$$T = L / AR \tag{3}$$

(Obviously time T needed for advancing length L must be equal to L/AR. This also applies to walking at speed AR)

By simple substitution we have the following:

$$T = L / (PR \times T^m)$$

(Here, T appears on both sides of equation: the final expression for T is therefore:)

$$T = (L/PR)^{1/(1+m)} \tag{4}$$

This is a very important equation for TBM, if one accepts the case record evidence that (-) *m* is strongly related to low Q-values in fault zones and significant weakness zones. It is important because very *negative* (-) *m* values make the component $(1/(1+m))$ *too big*. So far this has not been acknowledged by the TBM industry.

If the fault zone is wide (large L) and PR is low (grippers inefficient, water problems etc.) then L/PR may get too big to tolerate a big component $(1/(1+m))$ in equation 4. It is easy (in fact much too easy) to calculate an almost ‘infinite’ time for a fault zone using this ‘theoretical’ equation. The writer knows of four permanently buried, usually fault-destroyed, occasionally rock-burst destroyed TBM (Pont Ventoux, Dul Hasti, Pinglin, Jinping II). There are certainly many more, and the causes may be related to equation 4 logic: where Q is too low.

Figure 35 illustrates just two cases of fault zone delays, which have been explained in more detail by the original authors as cited under the figures. In the case of the Pinglin Tunnel, which had the tunnel name changed by order of the Taiwan president, the three TBM eventually all came to grief (one TBM getting crushed beneath a fault-zone collapse). Drill-and-blast NATM-style tunneling was needed to complete this ultra-challenging project, after many fatalities.

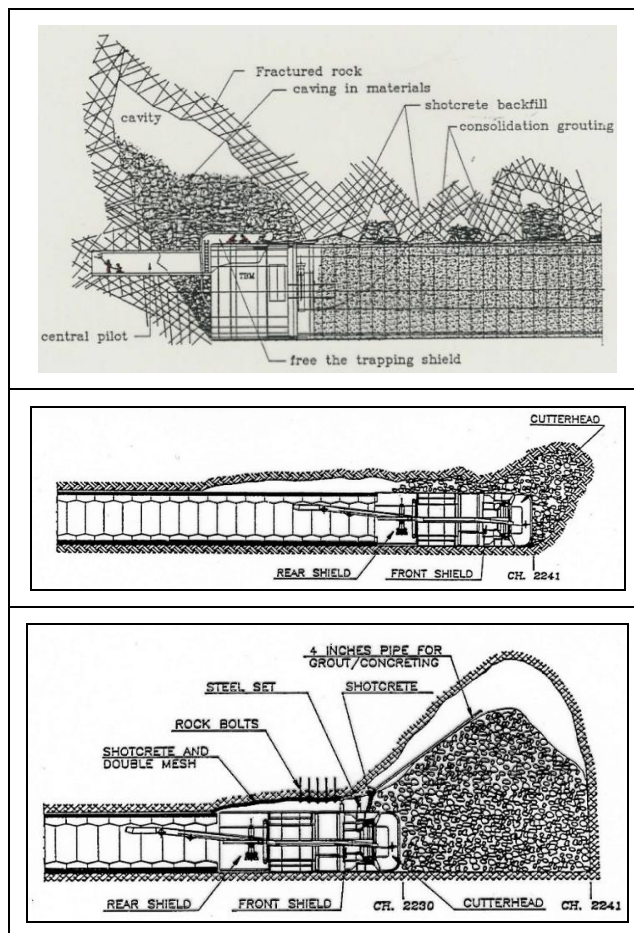


Figure 34. Some of the graphically-described challenges reported by Shen et al.(1999) and Grandori et al.(1995) at the Pinglin Road Tunnels in Taiwan, and at the Evinos Mornos water transfer project in Greece. Note – in retrospect – the disadvantage of releasing load on a fault zone by withdrawing the TBM. This causes a relatively lower seismic quality to become *extremely low* due to the release of stress. The fault then behaves as if encountered near the surface, with $V_p \approx 2\text{-}2.5$ km/s (Barton, 2006).

CONCLUSIONS

Tunnelling in *massive intact rock* at great depth may cause fracturing of the rock if the tangential stress reaches the magnitude of σ_v/v . The traditional ratio $\sigma_{\theta\max}/UCS > 0.4$ for increased SRF, or depth of failure, can therefore be further quantified by tensile strength and Poisson’s ratio. Fractures first develop due to extensional strain, then may propagate in shear which is unstable, and may cause rock bursting.

Tunnelling in *jointed rock* introduces another set of challenges which especially revolve around the number of joint sets and the joint roughness. When the ratio $J_n/J_r \geq 6$ over-break must be expected, but elevated J_a values representing clay-fillings might reduce this

ratio. Joint shearing due to water, clay-coatings, wedges and block size may dominate behaviour.

NMT, the Norwegian Method of Tunnelling, is basically a collection of economic single-shell B+S(fr) *help-the-rock-to-help-itself* solutions. Actual arching loads in the rock around tunnels dominate their stability. Over-break increases the amount of shotcrete, but filling with shotcrete or concrete is neither needed nor practiced. The use of lattice-girders should not be part of NMT as they are too deformable.

Tunnelling through *fault zones* with TBM causes delays and can draw-down water tables. TBM suffer time-dependent utilization. Even world records show this. Low Q-values are a specific cause of the deceleration (-m) gradient.

REFERENCES

- Addis, M.A., Barton, N., Bandis, S.C. & Henry, J.P. 1990. Laboratory studies on the stability of vertical and deviated boreholes. 65th Annual Technical Conference and Exhibition of the Society of Petroleum Engineers, New Orleans, September 23-26, 1990.
- Barton, N. & Hansteen, H. 1979. Very large span openings at shallow depth: Deformation magnitudes from jointed models and F.E. analysis. 4th RETC; Atlanta Georgia, Vol. 2: 1131-1353. Eds Maevis and Hustrulid. Am. Inst. of Min. & Metall., and Petr. Engrs, Inc. New York.
- Barton, N., Grimstad, E., Aas, G., Opsahl, O.A., Bakken, A., Pedersen, L. & Johansen, E.D. 1992. Norwegian Method of Tunnelling. WT Focus on Norway, World Tunnelling, June 6p. /August 5p. 1992.
- Barton, N. & Grimstad, E. 1994. The Q-system following twenty years of application in NMT support selection. *43rd Geomechanics Colloquy, Salzburg, Felsbau*, 6/94, 428-436.
- Barton, N. 2000. *TBM Tunnelling in Jointed and Faulted Rock*. 173p. Balkema, Rotterdam.
- Barton, N. 2006. *Rock Quality, Seismic Velocity, Attenuation and Anisotropy*. Taylor & Francis, UK & Netherlands, 729 p.
- Barton, N. 2007. Rock mass characterization for excavations in mining and civil engineering. Proc. of *Int. Workshop on Rock Mass Classification in Mining*, Vancouver.
- Barton, N. 2012a. Assessing Pre-Injection in Tunnelling. *Tunnelling Journal*, Dec.2011/Jan. 2012, pp. 44-50.
- Barton, N. 2012b. Reducing risk in long deep tunnels by using TBM and drill-and-blast methods in the same project – the hybrid solution. Keynote lecture. Risk in Underground Construction. Chinese Academy of Engineering. CSRME, Wuhan. *J. Rock Mech. and Geotech. Eng.*, 4(2): 115-126,
- Barton, N. 2013. TBM prognoses for open-gripper and double-shield machines: challenges and solutions for weakness zones and water. *Bergmekanikkdag, NFF, Oslo*, 21.1-21.17.
- Barton, N. and E. Grimstad, 2014. Q-system - An illustrated guide following 40 years in tunneling. Web site www.nickbarton.com, 43 pages, 79 figures and photos.
- Barton, N. and Shen, B. 2017. Risk of shear failure and extensional failure around over-stressed excavations in brittle rock, *Journal of Rock Mechanics and Geotechnical Engineering* <http://dx.doi.org/10.1016/j.jrmge.2016.11.004>.
- Barton, N. 2016. Cavern and Tunnel Failures due to Adverse Structural Geology. Keynote lecture, 2nd Int. ISRM Specialized. Conf. on Soft Rocks, Cartagena, Colombia. Keynote lecture. 18p.
- Barton, N. 2017. Minimizing the Use of Concrete in Tunnels and Caverns – Comparing NATM and NMT. Keynote lecture, GeoMEast2017 Int. Conf. on Sustainable Civil Infrastructures (SCI): Innovative Infrastructure Geotechnology. Sharm El-Sheikh, Egypt, 36p.
- Bray, J.W. 1967. A study of jointed and fractured rock. Part I. Fracture patterns and their failure characteristics. *Felsmechanik*, V/2-3, 117-136.
- Grandori, R., Jaeger, M., Antonini, F. & Vigl, L. 1995. Evinos-Mornos Tunnel - Greece. Construction of a 30 km long hydraulic tunnel in less than three years under the most adverse geological conditions. Proc. RETC. San Francisco, CA. Williamson & Gowring (eds). 747-767. Littleton, CO: Soc. for Mining, Metallurgy, and Exploration, Inc.
- Grimstad, E. & Barton, N. 1993. Updating of the Q-System for NMT. Proceedings of the International Symposium on Sprayed Concrete - Modern Use of Wet Mix Sprayed Concrete for Underground Support, Fagernes, 1993, (Eds Kompen, Opsahl and Berg. Norwegian Concrete Association, Oslo, pp. 46-66.
- Hoek, E. and Brown, E. 1980. Underground excavations in rock. *Institution of Mining and Metallurgy*, 527p.
- Martin C D, Kaiser PK, McCreath D R. Hoek-Brown parameters for predicting the depth of brittle failure around tunnels. *Can. Geotech. J.*, 1999; 36:136-151.
- Shen, C.P., Tsai, H.C., Hsieh, Y.S. & Chu, B. 1999. The methodology through adverse geology ahead of Pinglin large TBM. *Proc. RETC. Orlando, FL*. Hilton & Samuelson (eds). Ch.8: 117-137. Littleton, CO: Soc. for Mining, Metallurgy, and Exploration, Inc
- Shen, B. & Barton, N. 1997. The disturbed zone around tunnels in jointed rock masses. *Technical Note, Int. J. Rock Mech. Min. Sci.*, Vol. 34: 1: 117-125.
- Shen B, Stephansson O, Rinne M. *Modelling Rock Fracturing Processes: A Fracture Mechanics Approach Using FRACOD*. Springer (publisher), 2014; 173p.
- Siren, T. (2012) *Fracture Toughness Properties of Rocks in Olkiluoto: Laboratory Measurements 2008–2009*, Posiva Report 2012-25.
- Sundaram, N.M. & Rafek, A.G. 1998. The influence of rock mass properties in the assessment of TBM performance. Proc. 8th IAEG congress, Vancouver. Moore & Hungr (eds). 3553-3559. Balkema.
- Vandevall, M. (1990). *Dramix - Tunnelling the World*. NV Bækert S.A, 1991 edition.
- Ward, W.H., Todd, P. and Berry, N.S.M. 1983. The Kielder Experimental Tunnel: Final Results. *Geotechnique* 33, 3, 275-291.